Journal of Japan Association for Earthquake Engineering, Vol. 20, No. 8, 2020

EXAMINATION OF AVERAGED STRESS DROP EQUATIONS CONNECTING OUTER AND INNER FAULT PARAMETERS FOR STRONG MOTION PREDECTION

Kazuo DAN[1], Masanobu TOHDO[2] and Atsuko OANA[3]

[1] Member, Dr. Eng., Ohsaki Research Institute, Inc.,
Tokyo, Japan, dan@ohsaki.co.jp
[2] Member, Dr. Eng., Ohsaki Research Institute, Inc.,
Tokyo, Japan, tohdo@ohsaki.co.jp
[3] Member, Dr. Eng., Ohsaki Research Institute, Inc.,
Tokyo, Japan, a.oana@ohsaki.co.jp

ABSTRACT: Averaged stress drop equations are important in fault modeling for predicting strong ground motions, because they relate the outer and inner fault parameters describing the asperity model. We examined several equations, including an equation of a buried circular crack by using the seismic moment, the area of the asperities, and the stress drop on the asperities. We compared the relationships between the seismic moment and the seismic fault area calculated by each equation with the existing empirical relationships, and concluded that the equation of a buried circular crack can be applied to small crustal and subduction plate-boundary earthquakes without surface breakings such as the May 1997 Kagoshima-ken Hokuseibu earthquake (M_W 6.1) and the 2003 Tokachi-oki earthquake (M_W 8.1). Most of the results showed that the equation of a buried circular crack cannot be applied to large crustal or subduction plate-boundary earthquakes with surface breakings such as the 2016 Kumamoto earthquake (M_W 7.1) and the 2011 off the Pacific coast of Tohoku earthquake (M_W 9.0). This is because the equation of a buried circular crack was derived from the fault model without surface breakings. Our examinations showed that the stress drop equation by Fujii and Matsu'ura (2000) and the dynamic stress drop equation by Irie et al. (2011) for a vertical strike-slip fault can be applied to the Kumamoto earthquake and that the dynamic stress drop equation by Dorjpalam et al. (2015) for a thrust fault can be applied to the Tohoku earthquake.

Keywords: Crustal earthquake, Subduction plate-boundary earthquake, Strong motion prediction, Outer fault parameter, Inner fault parameter, Surface fault breaking, Averaged stress drop equation

1. INTRODUCTION

In the official procedure for predicting strong ground motions, called Recipe, by the Headquarters for Earthquake Research Promotion (2016)[1)], hereafter HERP, the averaged stress drop is calculated by the

equation for a buried circular crack of Eshelby (1957)[2], and this leads to unrealistic fault parameters, such as the asperity area over 50% of the entire fault area, when the fault length gets longer. This is because the averaged stress drop equation for a buried circular crack cannot be applied to long faults with surface breakings (Dan et al., 2011)[3]. For this case, the Recipe by the HERP suggests a tentative adoption of 3.1 MPa as the averaged stress drop which was derived by Fujii and Matsu'ura (2000)[4] for vertical strike-slip fault earthquakes with surface breakings. Although the averaged stress drop equations are important because they relate the outer and inner fault parameters describing the asperity model, they have not been examined in detail so far.

Hence, we examined whether each of several equations of calculating the averaged stress drop is appropriate or not by checking that the seismic fault area (fault ruptured area located within the seismogenic layer), which is calculated from the seismic moment (one of the outer fault parameters) and the asperity area and stress drop (two of the inner fault parameters) by the equation, is consistent with the existing empirical relationships between the seismic moment and the seismic fault area.

Our targets are four types of earthquakes: 1) the March 1997 Kagoshima-ken Hokuseibu earthquake (M_W6.1), the 1997 Yamaguchi-ken Hokubu earthquake (M_W5.8), the 2004 Chuetsu earthquake (M_W6.6), the 2004 Rumoi-shicho earthquake (M_W 5.7), and the 2016 Tottori-ken Chubu earthquake (M_W 6.2) as crustal earthquakes without surface breakings, 2) the 2016 Kumamoto earthquake (M_W 7.1) as a crustal earthquake with surface breakings, 3) the 2003 Tokachi-oki earthquake (M_W 8.1) as a subduction plate-boundary earthquake without surface (sea bottom) breakings, and 4) the 2011 off the Pacific coast of Tohoku earthquake (M_W 9.0) as a subduction plate-boundary earthquake with surface (sea bottom) breakings.

Hereafter, we call an earthquake without ground surface breakings (or sea bottom breakings) a small earthquake and an earthquake with them a large earthquake, according to Scholz (2002)[5]. Some papers we referred to in this paper derived SMGA (Strong Motion Generation Area) areas and stress drops. However, we replaced them by asperity areas and stress drops, because Boatwright (1988)[6] had shown that the asperity with the high stress drop corresponds to the SMGA by the dynamic fault rupturing simulations.

2. CALCULATION EQUATIONS OF AVERAGED STATIC OR DYNAMIC STRESS DROP

In this Chapter, we compiled equations for calculating the averaged stress drop or averaged dynamic stress drop. Since our targets are fault models with finite lengths, we excluded the averaged stress drop equations for a buried vertical strike-slip fault with infinite length (Knopoff, 1957)[7] or for a buried vertical reverse fault with infinite length (Starr, 1928)[8].

2.1 Buried circular crack (Eshelby, 1957)[2]

Eshelby (1957)[2] obtained the equation for calculating the averaged stress drop $\Delta\sigma$ for a buried circular crack, whose circumference has no slip, as follows:

$$\Delta\sigma = (7/16)M_0/(S/\pi)^{3/2}. \quad (1)$$

Here, M_0 is the seismic moment, and S is the seismic fault area.

2.2 Vertical strike-slip equivalent semi-ellipsoidal crack with surface breakings (Watanabe et al., 1998)[9]

Watanabe et al. (1998)[9] obtained the equation for calculating the averaged stress drop $\Delta\sigma$ for a vertical strike-slip equivalent semi-ellipsoidal crack with surface breakings as follows:

$$\Delta\sigma = \begin{cases} \pi^{1/2}k[3/\{4(1-v)\}][E_{s1} + \{vk^2/(k^2-4)\}(K_{s1} - E_{s1})]M_0/L^3 & (k < 2) \\ (3/8)\pi^{3/2}\{(2-v)/(1-v)\}M_0/L^3 & (k = 2) \\ (\pi^{1/2}/2)k^2(3/4)[E_{s2} + \{v/(1-v)\}\{4/(k^2-4)\}(K_{s2} - E_{s2})]M_0/L^3 & (k > 2). \end{cases} \quad (2)$$

Here, L is the fault length, k is the aspect ratio $k = L/W$, W is the fault width, v is the Poisson ratio of the medium at the source (seismogenic layer). $K_{s1} = K[(1-k^2/4)^{1/2}]$, $E_{s1} = E[(1-k^2/4)^{1/2}]$, $K_{s2} = K[(1-4/k^2)^{1/2}]$, $E_{s2} = E[(1-4/k^2)^{1/2}]$, and K is the first kind of the ellipsoidal integration and E is the second kind. Equation (2) is supposed to be applied to crustal earthquakes.

2.3 Vertical strike-slip fault with surface breakings (Fujii and Matsu'ura, 2000)[4)]

Fujii and Matsu'ura (2000)[4)] obtained the equation for calculating the averaged stress drop $\Delta\sigma$ for a vertical strike-slip faults with surface breakings by the dynamic fault rupturing simulation as follows:

$$\Delta\sigma = [(aS + bW_{max})/S^2]M_0, \quad a = 0.014(1/\mathrm{km}), \quad b = 1. \quad (3)$$

Here, W_{max} is the seismic fault width (equal to the thickness of the seismogenic layer). They showed that its appropriate value is W_{max} = 12 km for crustal earthquakes at plate boundaries, and W_{max} = 15 km for crustal earthquakes inside plates.

2.4 Vertical strike-slip fault with surface breakings (Irie et al., 2011)[10)]

Irie et al. (2011)[10)] obtained the equation for calculating the averaged dynamic stress drop $\Delta\sigma^{\#}$ for a vertical strike-slip fault with surface breakings by the dynamic fault rupturing simulation as follows:

$$\Delta\sigma^{\#} = cM_0/SW_{max}, \quad c = 0.5 + 2\exp[-L/W_{max}]. \quad (4)$$

Here, c is the geometric stress constant which is a function of the aspect ratio L/W_{max}. W_{max} is the seismic fault width (equal to the thickness of the seismogenic layer), and its value was assumed to be 15 km. Equation (4) was supposed to be applied to crustal earthquakes.

2.5 Thrust fault with surface breakings (Dorjpalam et al., 2015)[11)]

Dorjpalam et al. (2015)[11)] obtained the equation for calculating the averaged dynamic stress drop $\Delta\sigma^{\#}$ for a thrust fault dipping δ = 15° with surface (sea bottom) breakings as follows:

$$\Delta\sigma^{\#} = cM_0/SW_{max}, \quad c = 0.45 + 1.1\exp[-L/W_{max}]. \quad (5)$$

Here, W_{max} is the seismic fault width and written by W_{max} = thickness of the seismogenic layer/sinδ. W_{max} was set to be 200 km (thickness of the seismogenic layer is 51.8 km) in their dynamic fault rupturing simulation. Equation (5) was supposed to be applied to subduction plate-boundary earthquakes.

3. CALCULATION EQUATIONS OF THE SEISMIC FAULT AREA

In this Chapter, we derive equations for calculating the seismic fault area S from the seismic moment M_0, the asperity area S_{asp}, and the asperity stress drop $\Delta\sigma_{asp}$ by using the averaged stress drop equations compiled in Chapter 2.

3.1 Buried circular crack (Eshelby, 1957)[2)]

The averaged stress drop $\Delta\sigma$ of the asperity model is described by

$$\Delta\sigma = \sum_i S_{aspi}\Delta\sigma_{aspi}/S. \quad (6)$$

Here, S_{aspi} and $\Delta\sigma_{aspi}$ are the area and the stress drop of the i-th asperity, respectively. For a buried circular crack, the seismic fault area S can be calculated from M_0, S_{aspi}, and $\Delta\sigma_{aspi}$ by Eqs. (1) and (6) as follows:

$$S = (7/16)^2\pi^3(M_0/\sum_i S_{aspi}\Delta\sigma_{aspi})^2. \quad (7)$$

The averaged stress drop $\Delta\sigma$ can be obtained by substituting the seismic fault area S calculated by Eq. (7) to Eq. (6).

3.2 Vertical strike-slip equivalent semi-ellipsoidal crack with surface breakings (Watanabe et al., 1998)[9)]

For the vertical strike-slip equivalent semi-ellipsoidal crack with surface breakings, the seismic moment is described from Eqs. (2) and (6) as follows:

$$M_0 = \begin{cases} \pi^{-1/2}k^{-1}[\{4(1-v)\}/3]L^3\sum_i S_{aspi}\Delta\sigma_{aspi}/S\,/[E_{s1}+\{vk^2/(k^2-4)\}(K_{s1}-E_{s1})] & (k<2) \\ (8/3)\pi^{-3/2}\{(1-v)/(2-v)\}L^3\sum_i S_{aspi}\Delta\sigma_{aspi}/S & (k=2) \\ (2/\pi^{1/2})k^{-2}(4/3)L^3\sum_i S_{aspi}\Delta\sigma_{aspi}/S\,/[E_{s2}+\{v/(1-v)\}\{4/(k^2-4)\}(K_{s2}-E_{s2})] & (k>2). \end{cases} \quad (8)$$

Since Eq. (2) is for a vertical fault, we can assume the seismic fault width W to be equal to the thickness of the seismogenic layer W_{max} and then the unknown parameter is the seismic fault length L only. Hence, we change the value of L from small to large to find a suitable length L so that the seismic moment M_0 by Eq. (8) matches the given seismic moment of each target event. The averaged stress drop $\Delta\sigma$ can be obtained by substituting the suitable length L to Eq. (2).

Note here that the seismic moment M_0 by Eq. (8) converges on $\{8/(3\pi^{1/2})\}W_{max}\sum_i S_{aspi}\Delta\sigma_{aspi}$ for large L and that we cannot obtain a suitable length L when the given seismic moment M_0 is larger than this upper limit.

3.3 Vertical strike-slip fault with surface breakings (Fujii and Matsu'ura, 2000)[4)]

For the vertical strike-slip fault with surface breakings examined by Fujii and Matsu'ura (2000)[4)], the seismic fault area S can be calculated from M_0, S_{aspi}, and $\Delta\sigma_{aspi}$ by Eqs. (3) and (6) as follows:

$$S = bW_{max}M_0/[\sum_i S_{aspi}\Delta\sigma_{aspi} - aM_0]. \quad (9)$$

The averaged stress drop $\Delta\sigma$ can be obtained by substituting S in Eq. (9) to Eq. (3).

Note here that the seismic moment M_0 is written by

$$M_0 = \sum_i S_{aspi}\Delta\sigma_{aspi}/(a + b\ W_{max}/S). \quad (10)$$

from Eqs. (3) and (6), that the seismic moment M_0 converges on $\sum_i S_{aspi}\Delta\sigma_{aspi}/a$ for large S, and that we cannot obtain a suitable seismic fault area S when the given seismic moment M_0 is larger than this upper limit.

3.4 Vertical strike-slip fault with surface breakings (Irie et al., 2011)[10)]

For the vertical strike-slip fault with surface breakings examined by Irie et al. (2011)[10)], the seismic fault area S can be calculated from M_0, S_{aspi}, and $\Delta\sigma_{aspi}$ by Eqs. (4) and (6) as follows:

$$S = -W_{max}^2 \log[\, W_{max} \sum_i S_{aspi} \Delta\sigma_{aspi} / (2M_0) - 0.25]. \quad (11)$$

Here, we assumed that the averaged stress drop $\Delta\sigma$ should be equal to the averaged dynamic stress drop $\Delta\sigma^{\#}$. The averaged dynamic stress drop $\Delta\sigma^{\#}$ can be obtained by substituting S in Eq. (11) to Eq. (4).

Note here that the seismic moment M_0 is written by

$$M_0 = W_{max} \sum_i S_{aspi} \Delta\sigma_{aspi} / (0.5 + 2 \exp[-L/W_{max}]) \quad (12)$$

from Eqs. (4) and (6), that the seismic moment M_0 converges on $W_{max}\sum_i S_{aspi}\, \Delta\sigma_{aspi}/2.5$ for small L and on $2W_{max}\sum_i S_{aspi}\, \Delta\sigma_{aspi}$ for large L, and that we cannot obtain a suitable seismic fault area S when the given seismic moment M_0 is not in the range between $W_{max}\sum_i S_{aspi}\, \Delta\sigma_{aspi}/2.5$ and $2W_{max}\sum_i S_{aspi}\, \Delta\sigma_{aspi}$.

3.5 Thrust fault with surface breakings (Dorjpalam et al., 2015)[11)]

For the thrust fault with surface breakings examined by Dorjpalam et al. (2015)[11)], the seismic fault area S can be calculated from M_0, S_{aspi}, and $\Delta\sigma_{aspi}$ by Eqs. (5) and (6) as follows:

$$S = -W_{max}^2 \log[\, W_{max} \sum_i S_{aspi} \Delta\sigma_{aspi} / (1.1M_0) - 0.41]. \quad (13)$$

Here, we assumed that the averaged stress drop $\Delta\sigma$ should be equal to the averaged dynamic stress drop $\Delta\sigma^{\#}$. The averaged dynamic stress drop $\Delta\sigma^{\#}$ can be obtained by substituting S in Eq. (13) to Eq. (5).

Note here that the seismic moment M_0 is written by

$$M_0 = W_{max} \sum_i S_{aspi} \Delta\sigma_{aspi} / (0.45 + 1.1 \exp[-L/W_{max}]) \quad (14)$$

from Eqs. (5) and (6), that the seismic moment M_0 converges on $W_{max}\sum_i S_{aspi}\, \Delta\sigma_{aspi}/1.55$ for small L and on $2.22W_{max}\sum_i S_{aspi}\, \Delta\sigma_{aspi}$ for large L, and that we cannot obtain a suitable seismic fault area S when the given seismic moment M_0 is not in the range between $W_{max}\sum_i S_{aspi}\, \Delta\sigma_{aspi}/1.55$ and $2.22W_{max}\sum_i S_{aspi}\, \Delta\sigma_{aspi}$.

4. CALCULATION RESULTS OF THE SEISMIC FAULT AREAS

4.1 Crustal earthquakes without surface breakings

In this Section, we examined crustal earthquakes caused by buried faults of the March 1999 Kagoshima-ken Hokuseibu earthquake (M_W 6.1), the 1997 Yamaguchi-ken Hokubu earthquake (M_W 5.8), the 2004 Chuetsu earthquake (M_W 6.6), the 2004 Rumoi-shicho earthquake (M_W 5.7), and the 2016 Tottori-ken Chubu earthquake (M_W 6.2). Only Eq. (1) for a buried circular crack, out of the five equations compiled in Chapter 2, can be applied to earthquakes by buried faults.

Tables 1 to 5 list the outer and inner fault parameters (Miyake et al., 2003; Shimazu et al., 2009; Kamae et al., 2005; Maeda and Sasatani, 2009; Yoshida et al., 2018)[12)–16)], used as input data in this study, and the calculation results of the averaged stress drop $\Delta\sigma$, the seismic fault area S, and the asperity area ratio S_{asp}/S. In Table 5, * shows that the calculation results are invalid because of S_{asp}/S over 0.5 (Dan et al., 2011)[3)] (same in Tables 6 and 8).

These tables show that the averaged stress drops $\Delta\sigma$ are from 1.16 to 3.23 MPa except for Tottori-ken Chubu earthquake which was excluded because of S_{asp}/S over 0.5 and that these values are in the range of 0.5 to 2 times of $\Delta\sigma$ = 2.3 MPa which is obtained by Eq. (1) and the empirical relationship of Somerville et al. (1999)[17)] between the seismic moment and the seismic fault area. The asperity area ratios S_{asp}/S are from 0.11 to 0.34, and these values are in the range of 0.5 to 2 times of S_{asp}/S = 0.22 which was obtained by Somerville et al. (1999)[17)] from the slip inversion results of the 15 crustal earthquakes.

Table 1 Fault parameters of the March 1997 Kagoshima-ken Hokuseibu earthquake and calculation results

outer fault parameter (F-net, 1997)	seismic moment M_0	1.40×10^{18} N·m
inner fault parameters and short-period level (Miyake et al., 2003)[12]	combined asperity area S_{asp}	$S_{asp\,1} = 42$ km^2
	asperity stress drop $\Delta\sigma_{asp}$	$\Delta\sigma_{asp\,1} = 7.29$ MPa
	short-period level A	3.22×10^{18} N·m/s^2
results by equation (1) for a buried circular crack	averaged stress drop $\Delta\sigma$	2.47 MPa
	seismic fault area S	124 km^2
	asperity area ratio S_{asp}/S	0.34

Table 2 Fault parameters of the 1997 Yamaguchi-ken Hokubu earthquake and calculation results

outer fault parameter (F-net, 1997)	seismic moment M_0	5.66×10^{17} N·m
inner fault parameters and short-period level (Shimazu et al., 2009)[13]	combined asperity area S_{asp}	$S_{asp\,1} = 14.4$ km^2
	asperity stress drop $\Delta\sigma_{asp}$	$\Delta\sigma_{asp\,1} = 7.4$ MPa
	short-period level A	1.92×10^{18} N·m/s^2
results by equation (1) for a buried circular crack	averaged stress drop $\Delta\sigma$	1.16 MPa
	seismic fault area S	112 km^2
	asperity area ratio S_{asp}/S	0.11

Table 3 Fault parameters of the 2004 Chuetsu earthquake and calculation results

outer fault parameter (F-net, 2004)	seismic moment M_0	7.53×10^{18} N·m
inner fault parameters and short-period level (Kamae et al., 2005)[14]	combined asperity area $S_{asp} = 91$ km^2	$S_{asp\,1} = 75$ km^2
		$S_{asp\,2} = 16$ km^2
	asperity stress drop $\Delta\sigma_{asp}$	$\Delta\sigma_{asp\,1} = 7$ MPa
		$\Delta\sigma_{asp\,2} = 20$ MPa
	short-period level A	8.72×10^{18} N·m/s^2
results by equation (1) for a buried circular crack	averaged stress drop $\Delta\sigma$	1.79 MPa
	seismic fault area S	471 km^2
	asperity area ratio S_{asp}/S	0.16

Table 4 Fault parameters of the 2004 Rumoi-shicho earthquake and calculation results

outer fault parameter (F-net, 2004)	seismic moment M_0	4.44×10^{17} N·m
inner fault parameters and short-period level (Maeda and Sasatani, 2009)[15]	combined asperity area $S_{asp} = 9.8$ km^2	$S_{asp\,1} = 1.96$ km^2
		$S_{asp\,2} = 7.84$ km^2
	asperity stress drop $\Delta\sigma_{asp}$	$\Delta\sigma_{asp\,1} = 27.9$ MPa
		$\Delta\sigma_{asp\,2} = 12.9$ MPa
	short-period level A	3.39×10^{18} N·m/s^2
results by equation (1) for a buried circular crack	averaged stress drop $\Delta\sigma$	3.23 MPa
	seismic fault area S	48 km^2
	asperity area ratio S_{asp}/S	0.20

Table 5 Fault parameters of the 2016 Tottori-ken Chubu earthquake and calculation results

outer fault parameter (F-net, 2016)	seismic moment M_0	2.24×10^{18} N·m
inner fault parameters and short-period level (Yoshida et al., 2018)[16]	combined asperity area $S_{asp} = 50.9$ km^2	$S_{asp\,1} = 38.9$ km^2
		$S_{asp\,2} = 12.0$ km^2
	asperity stress drop $\Delta\sigma_{asp}$	$\Delta\sigma_{asp\,1} = 14.3$ MPa
		$\Delta\sigma_{asp\,2} = 7.6$ MPa
	short-period level A	8.08×10^{18} N·m/s^2
results by equation (1) for a buried circular crack	averaged stress drop $\Delta\sigma$	9.12 MPa
	seismic fault area S	71 km^2
	asperity area ratio S_{asp}/S	0.72*

*: invalid because of S_{asp}/S over 0.5 (Dan et al., 2011).

Figure 1 shows the calculated seismic fault areas, with the seismic moments, of the four earthquakes out of five earthquakes, excluding the result of the Tottori-ken Chubu earthquake with the asperity area ratio S_{asp}/S beyond 0.5. This figure also shows the empirical relationship between the seismic fault area and the seismic moment adopted in the Recipe by HERP (2016)[1]. This empirical relationship consists of three lines: the first stage ($M_0 < 7.5 \times 10^{18}$ N·m) where the ruptured fault does not reach the ground surface and the fault length, the width, and the slip are proportional to each other, the second stage (7.5×10^{18} N·m $\leq M_0 \leq 1.8 \times 10^{20}$ N·m) where the ruptured fault reaches the ground surface and the fault width saturates, and the third stage (1.8×10^{20} N·m $< M_0$) where the slip also saturates. We also show its half and double lines in order to judge the applicability of the averaged stress drop equations. Figure 1 indicates that the seismic fault areas calculated by Eq. (1) for a buried circular crack are consistent with the empirical relationship adopted in the Recipe.

Figure 2 shows the short-period level A calculated from the asperity area S_{aspi} and the asperity stress drop $\Delta\sigma_{aspi}$ for all the fault models in this study by the following equation:

$$A = [\sum_i \{4\pi\beta^2 \Delta\sigma_{aspi} (S_{aspi}/\pi)^{1/2}\}^2]^{1/2}. \quad (15)$$

Here, β is the S-wave velocity at the source (seismogenic layer), and its value was taken from each reference of the inner fault parameters. Figure 2 also shows the empirical relationship by Dan et al. (2001)[18] between the seismic moment and the short-period level, adopted in the Recipe of HERP, and its half and double lines. The solid parts show the range of the seismic moments of the crustal earthquakes used to obtain the empirical relationship, and the dotted parts show the ranges out of the seismic moments. Figure 2 indicates that all the short-period levels of the fault models in this study are within the range of 1/2 to 2 times of the empirical relationship by Dan et al. (2001)[18].

Our results show that Eq. (1) for a buried crack model is suitable for calculating the averaged stress drop of crustal earthquakes without surface breakings.

4.2 Crustal earthquake with surface breakings

In this Section, we examined a crustal earthquake with surface breakings of the 2016 Kumamoto earthquake (M_W 7.1). Here, although Eq. (1) is for a buried circular crack and it cannot be applied to second-stage earthquakes with surface breakings, we applied it to the Kumamoto earthquake, one of the

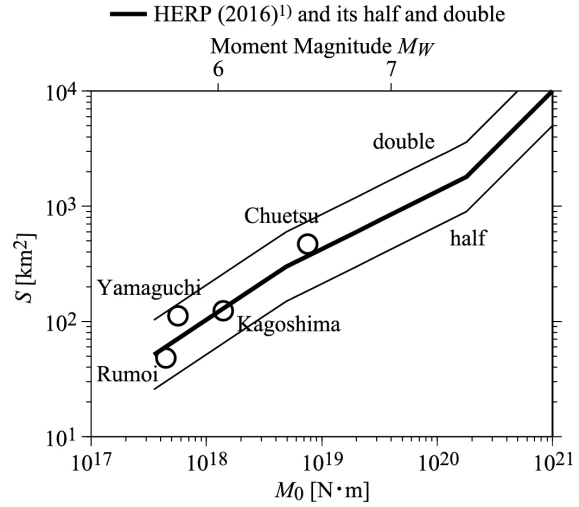

Fig. 1 Relationship between the seismic moment and the seismic fault area calculated by Eq. (1) for a buried circular crack in the case of crustal earthquakes without surface breakings.

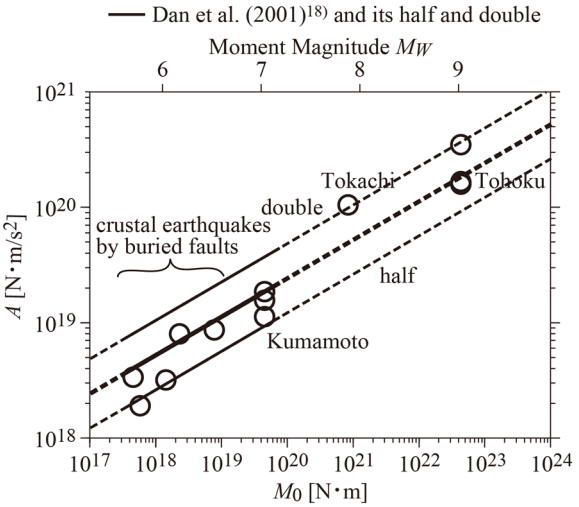

Fig. 2 Relationship between the seismic moment and the short-period level calculated from the inner fault parameters of the earthquakes examined in this study

second-stage earthquakes, and examined its applicability, because HERP (2016)[1] applies it to the second-stage earthquakes in the Recipe. We assumed W_{max} = 15 km for the Kumamoto earthquake because Fujii and Matsu'ura (2000)[4] assumed W_{max} = 15 km for crustal earthquakes inside the plates, Irie et al. (2011)[10] also assumed W_{max} = 15 km in their dynamic fault rupturing simulation, and Irikura et al. (2017)[19] set the fault width to be 18 km for the Kumamoto earthquake and the upper depth of the seismogenic layer is 3 km in Kumamoto region (HERP, 2014)[20].

The dip of the faults for the Kumamoto earthquake by Irikura et al. (2017)[19] is from 65° to 77°, while Fujii and Matsu'ura (2000)[4] and Irie et al. (2011)[10] assumed vertical faults dipping 90°.

Table 6 lists the inner fault parameters of the 2016 Kumamoto earthquake obtained by Irikura et al. (2017)[19], Satoh (2017)[21], and Oana et al. (2017)[22] and our calculation results. Here, Irikura et al. (2017)[19] proposed a source model consisting of three asperities in order to reproduce strong motions and a simplified source model consisting one asperity in order to validate the simplified source model for strong motion prediction, and we adopted the former because we prioritized the reproducibility of the strong motions. Note here that we could not obtain a suitable seismic fault length L when we applied Eq. (2) for a vertical strike-slip equivalent ellipsoidal crack with surface breakings to the inner fault parameters by Oana et al. (2017)[22] because the seismic moment did not reach 4.42×10^{19} N·m for large seismic fault length L under condition of W_{max} = 15 km.

Table 6 shows that the averaged stress drop $\Delta\sigma$ calculated by Eq. (1) for a buried circular crack are from 0.64 MPa to 5.69 MPa except for the cases of S_{asp}/S over 0.5 and that those by Eqs. (2) to (4) for a vertical strike-slip fault with surface breakings are from 3.44 to 3.91 MPa, which are close to $\Delta\sigma$ = 3.1 MPa obtained by Fujii and Matsu'ura (2000)[4] and $\Delta\sigma$ = 3.4 MPa obtained by Dan et al. (2011)[3]. The asperity area ratios S_{asp}/S calculated by Eq. (1) for a buried circular crack are from 0.072 to 0.49 and those by Eqs. (2) and (4) are from 0.072 to 0.49, which are in the range of 1/2 to 2 times of S_{asp}/S = 0.22 obtained by Somerville et al. (1999)[17].

Figure 3 shows the seismic moment and the seismic fault area calculated by Eq. (1) for a buried circular crack. Figure 3 also shows empirical relationships between the seismic moment and the seismic fault area proposed by Fujii and Matsu'ura (2000)[4] and Dan et al. (2011)[3] for the second- and third-stage earthquakes as well as the empirical relationship by the HERP (2016)[1]. Here, the seismic fault area S within the seismogenic layer, not fault ruptured area S_{rup}, is plotted for the empirical relationship by Dan et al. (2011)[3]. It is found out that the empirical relationships by Fujii and Matsu'ura (2000)[4] and Dan et al. (2011)[3] are in the range of 1/2 to 2 times of that by the HERP (2016)[1].

Figure 3 indicates that the seismic fault areas calculated from the inner fault parameters of Irikura et al. (2017)[19] and Oana et al. (2017)[22] by Eq. (1) for a buried circular crack are rather larger than the existing empirical relationships and that the seismic fault area calculated from the inner fault parameters of Satoh (2017)[21] is consistent with the empirical relationships. This is because the calculated seismic fault area S is proportional to the square of the asperity area S_{aspi} as shown by Eq. (7) and the combined asperity area S_{asp} is 1.6 to 1.7 times larger than those of other two models.

Figure 4 shows the relationship between the seismic moment M_0 and the seismic fault area S calculated by Eq. (2) for a vertical strike-slip equivalent semi-ellipsoidal crack with surface breakings. It is clear that the seismic fault area S calculated from the inner fault parameters of Irikura et al. (2017)[19] by Eq. (2) for a vertical strike-slip equivalent semi-ellipsoidal crack agrees with the existing empirical relationships.

Figure 5 shows the relationship between the seismic moment M_0 and the seismic fault area S calculated by Eq. (3) for a vertical strike-slip fault with surface breakings. The figure indicates that the seismic fault area S from the inner fault parameters of Oana et al. (2017)[22] by Eq. (3) is consistent with the existing empirical relationships.

Figure 6 shows the relationship between the seismic moment M_0 and the seismic fault area S calculated by Eq. (4) for a vertical strike-slip fault with surface breakings. The figure indicates that the seismic fault area S from the inner fault parameters of Oana et al. (2017)[22] by Eq. (4) for a vertical strike-slip fault with surface breakings is consistent with the existing empirical relationships.

Our results show that the seismic fault area calculated from the inner fault parameters of Satoh (2017)[21] by Eq. (1) for a buried circular crack is consistent with the existing empirical relationships

while those from the inner fault parameters of Irikura et al. (2017)[19] and Oana et al. (2017)[22] are larger than the existing empirical relationships and that the seismic fault areas calculated from the inner fault parameters of Irikura et al. (2017)[19] and Oana et al. (2017)[22] by Eq. (2) for a vertical strike-slip equivalent semi-ellipsoidal crack with surface breakings and by Eqs. (3) and (4) for a vertical strike-slip fault with surface breakings are consistent with the empirical relationships by the HERP (2016)[1], Fujii and Matsu'ura (2000)[4], and Dan et al. (2011)[3]. We can summarize here that Eq. (1) for a buried circular crack may not be suitable to be applied to the 2016 Kumamoto earthquake with surface breakings.

Table 6 Fault parameters of the 2016 Kumamoto earthquake and calculation results

(a) outer fault parameter

outer fault parameter [F-net, 2016]	seismic moment M_0	4.42×10^{19} N·m

(b) inner fault parameters by Irikura *et al*. [2017] and the results

inner fault parameters and short-period level (Irikura *et al*., 2017)[19]	combined asperity area $S_{asp} = 203.6$ km^2	$S_{asp\,1} = 51.8$ km^2
		$S_{asp\,2} = 51.8$ km^2
		$S_{asp\,3} = 100$ km^2
	asperity stress drop $\Delta\sigma_{asp}$	$\Delta\sigma_{asp\,1} = 13.6$ MPa
		$\Delta\sigma_{asp\,2} = 13.6$ MPa
		$\Delta\sigma_{asp\,3} = 13.4$ MPa
	short-period level A	1.58×10^{19} N·m/s^2
results by equation (1) for a buried circular crack	averaged stress drop $\Delta\sigma$	1.79 MPa
	seismic fault area S	1,530 km^2
	asperity area ratio S_{asp}/S	0.13
results by equation (2) for a vertical strike-slip equivalent semi-ellipsoidal crack with surface breakings	averaged stress drop $\Delta\sigma$	3.62 MPa
	seismic fault area S	760 km^2
	asperity area ratio S_{asp}/S	0.27
results by equation (3) for a vertical strike-slip fault with surface breakings	averaged stress drop $\Delta\sigma$	8.83 MPa
	seismic fault area S	311 km^2
	asperity area ratio S_{asp}/S	0.65*
results by equation (4) for a vertical strike-slip fault with surface breakings	averaged dynamic stress drop $\Delta\sigma^{\#}$	7.98 MPa
	seismic fault area S	344 km^2
	asperity area ratio S_{asp}/S	0.59*

*: invalid because of S_{asp}/S over 0.5 (Dan et al., 2011)[3].

(c) inner fault parameters by Satoh (2017)[21] and the results

inner fault parameters and short-period level (Satoh, 2017)[21]	combined asperity area $S_{asp} = 351.36$ km^2	$S_{asp\,1} = 115.2$ km^2
		$S_{asp\,2} = 103.68$ km^2
		$S_{asp\,3} = 34.56$ km^2
		$S_{asp\,4} = 46.08$ km^2
		$S_{asp\,5} = 51.84$ km^2
	asperity stress drop $\Delta\sigma_{asp}$	$\Delta\sigma_{asp\,1} = 11.5$ MPa
		$\Delta\sigma_{asp\,2} = 11.5$ MPa
		$\Delta\sigma_{asp\,3} = 11.5$ MPa
		$\Delta\sigma_{asp\,4} = 11.5$ MPa
		$\Delta\sigma_{asp\,5} = 11.5$ MPa
	short-period level A	1.87×10^{19} N·m/s^2
results by equation (1) for a buried circular crack	averaged stress drop $\Delta\sigma$	5.69 MPa
	seismic fault area S	710 km^2
	asperity area ratio S_{asp}/S	0.49
results by equation (2) for a vertical strike-slip equivalent semi-ellipsoidal crack with surface breakings	averaged stress drop $\Delta\sigma$	10.8 MPa
	seismic fault area S	374 km^2
	asperity area ratio S_{asp}/S	0.94*
results by equation (3) for a vertical strike-slip fault with surface breakings	averaged stress drop $\Delta\sigma$	20.9 MPa
	seismic fault area S	194 km^2
	asperity area ratio S_{asp}/S	1.81*
results by equation (4) for a vertical strike-slip fault with surface breakings	averaged dynamic stress drop $\Delta\sigma^{\#}$	21.6 MPa
	seismic fault area S	187 km^2
	asperity area ratio S_{asp}/S	1.88*

*: invalid because of S_{asp}/S over 0.5 (Dan et al., 2011)[3].

(d) inner fault parameters by Oana et al. (2017)[22] and the results

inner fault parameters and short-period level (Oana et al., 2017)[22]	combined asperity area $S_{asp} = 220$ km^2	$S_{asp\,1} = 120$ km^2
		$S_{asp\,2} = 64$ km^2
		$S_{asp\,3} = 36$ km^2
	asperity stress drop $\Delta\sigma_{asp}$	$\Delta\sigma_{asp\,1} = 6$ MPa
		$\Delta\sigma_{asp\,2} = 13$ MPa
		$\Delta\sigma_{asp\,3} = 11$ MPa
	short-period level A	1.14×10^{19} N·m/s^2
results by equation (1) for a buried circular crack	averaged stress drop $\Delta\sigma$	0.64 MPa
	seismic fault area S	3,060 km^2
	asperity area ratio S_{asp}/S	0.072
results by equation (3) for a vertical strike-slip fault with surface breakings	averaged stress drop $\Delta\sigma$	3.91 MPa
	seismic fault area S	499 km^2
	asperity area ratio S_{asp}/S	0.44
results by equation (4) for a vertical strike-slip fault with surface breakings	averaged dynamic stress drop $\Delta\sigma^{\#}$	3.44 MPa
	seismic fault area S	567 km^2
	asperity area ratio S_{asp}/S	0.39

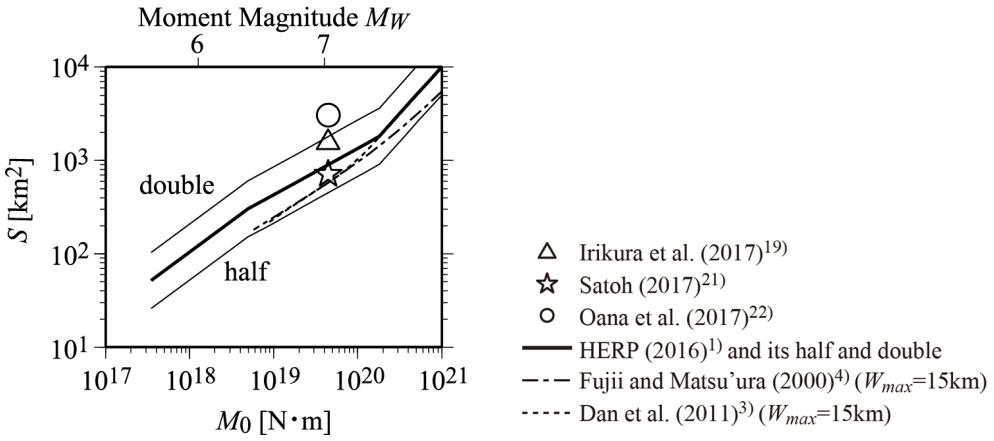

Fig. 3 Relationship between the seismic moment and the seismic fault area calculated from the inner fault parameters for the 2016 Kumamoto earthquake by Eq. (1) for a buried circular crack

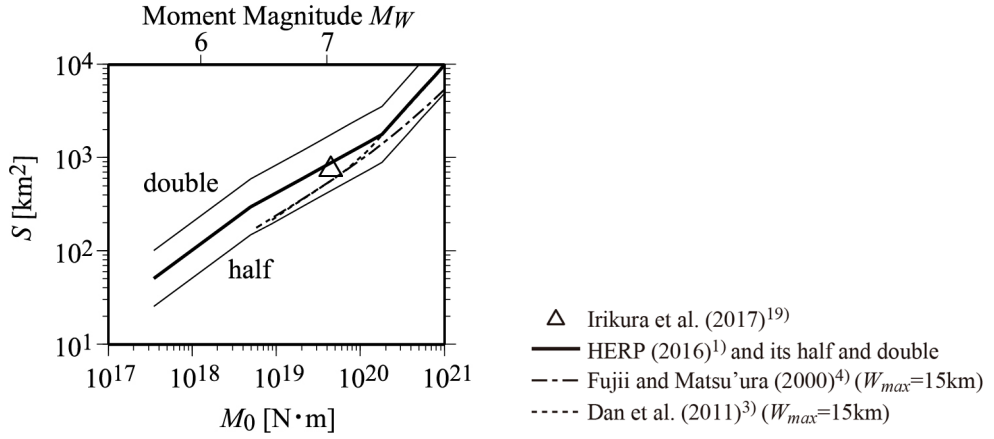

Fig. 4 Relationship between the seismic moment and the seismic fault area calculated from the inner fault parameters for the 2016 Kumamoto earthquake by Eq. (2) for a vertical strike-slip equivalent semi-ellipsoidal crack with surface breakings

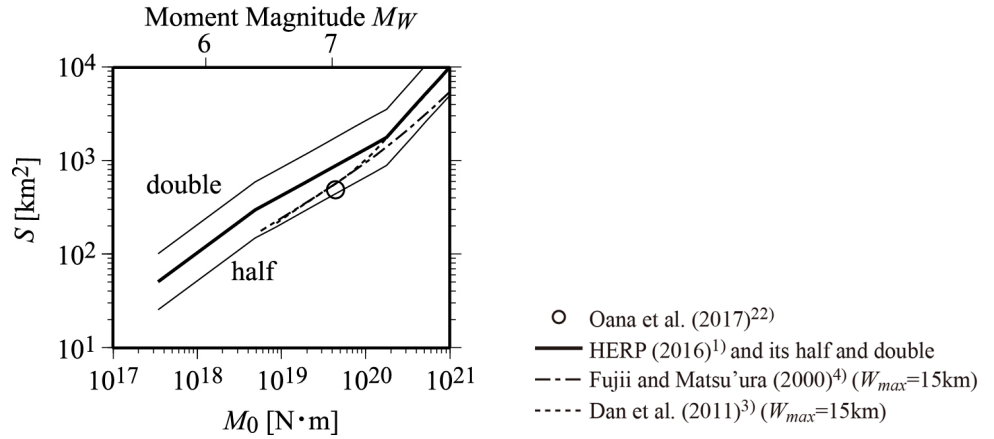

Fig. 5 Relationship between the seismic moment and the seismic fault area calculated from the inner fault parameters for the 2016 Kumamoto earthquake by Eq. (3) for a vertical strike-slip fault with surface breakings

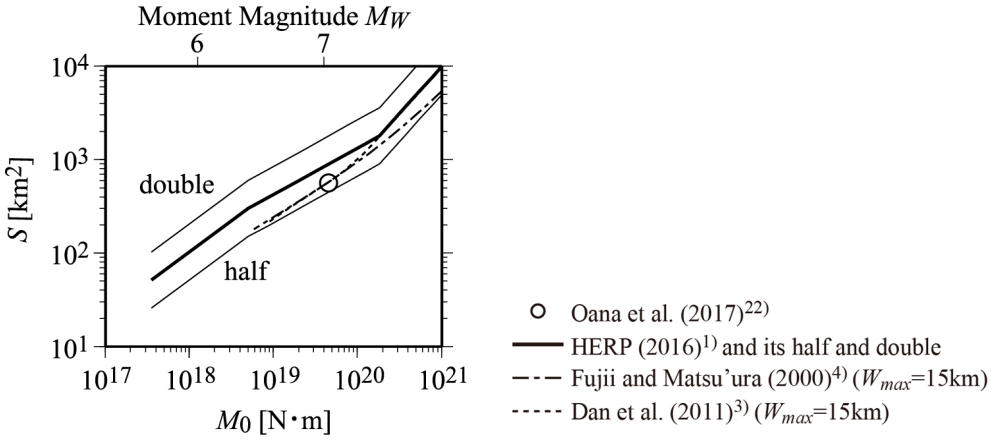

Fig. 6 Relationship between the seismic moment and the seismic fault area calculated from the inner fault parameters for the 2016 Kumamoto earthquake by Eq. (4) for a vertical strike-slip fault with surface breakings

4.3 Subduction plate-boundary earthquake without surface (sea bottom) breakings

In this Section, we examined a subduction plate-boundary earthquake without surface (sea bottom) breakings of the 2003 Tokachi-oki earthquake (M_W 8.1). This earthquake was caused by a thrust fault, and had little slip on the shallow part of the fault in the inversion results from long-period motions (e.g., Aoi et al., 2008)[23], and we have no report that any sea bottom breakings are discovered.

Table 7 lists the seismic moment and the inner fault parameters derived by Kamae and Kawabe (2004)[24] and our calculation results. The table shows that the averaged stress drop $\Delta\sigma$ is 10.5 MPa and it is about 3 times larger than $\Delta\sigma$ = 3.0 MPa calculated by Eq. (1) for a buried circular crack and empirical relationships between the seismic moment and the seismic fault area of Kanamori and Anderson (1975)[25] and Utsu (2001)[26]. The asperity area ratio is 0.42 and it is in the range of 1/2 to 2 times of S_{asp}/S = 0.25, which was obtained by Somerville et al. (2002)[27] from slip distributions of subduction plate-boundary earthquakes.

Figure 7 shows the seismic moment and the seismic fault area calculated by Eq. (1). The figure also shows the empirical relationship by Utsu (2001)[26], adopted in the Recipe, and its half and double. Here, the empirical relationship by Utsu (2001)[26] is supposed to be applied to first-stage subduction plate-boundary earthquakes, whose seismic fault length, width, and slip are proportional to each other, and the averaged stress drop is 3 MPa by Eq. (1) for a buried circular crack. However, the Recipe does not describe the upper limit of the seismic moment in the empirical relationship.

The figure indicates that the seismic fault area S calculated by Eq. (1) for a circular crack is consistent with the empirical relationship adopted by Recipe, and this means that Eq. (1) is suitable to calculate averaged stress drops of subduction plate-boundary earthquakes without surface (sea bottom) breakings.

4.4 Subduction plate-boundary earthquake with surface (sea bottom) breakings

In this Section, we examined a subduction plate-boundary earthquake with surface (see bottom) breakings of the 2011 off the Pacific coast of Tohoku earthquake. This earthquake was caused by a thrust fault. We assumed W_{max} = 200 km in the following calculation because W_{max} = 200 km was adopted in the dynamic fault rupturing simulation to obtain Eq. (5) and the fault width of the Tohoku earthquake was about 200 km (*e.g.*, Yoshida et al., 2011)[28].

Table 8 lists the inner fault parameters of the Tohoku earthquake obtained by Asano and Iwata (2012)[29], Satoh (2012)[30], Kawabe and Kamae (2013)[31], and Kurahashi and Irikura (2013)[32] and our calculation results. In the table, the seismic fault area S calculated from the inner fault parameters by

Satoh (2012)[30] by Eq. (5) for a thrust fault with surface breakings is 1/39.4 of the combined asperity area. This is because the seismic fault area by Eq. (13) gets small for a large asperity area S_{aspi} and large asperity stress drop $\Delta\sigma_{aspi}$ and because the combined asperity area of Satoh (2012)[30] is about 2 times larger than those of the three other models and the asperity stress drop is also about 1.5 times larger. This small seismic fault area leads to a quite large averaged stress $\Delta\sigma$ of 1,117 MPa.

Table 8 indicates that the averaged stress drop $\Delta\sigma$ calculated by Eq. (1) is in a wider range of 0.09 to 3.26 MPa except for the cases of S_{asp}/S over 0.5 and that the averaged dynamic stress drop $\Delta\sigma^{\#}$ calculated by Eq. (5) is in a narrower range of 0.48 to 1.44 MPa, which is in the range of 1/2 to 2 times of $\Delta\sigma^{\#} = 1.0$ MPa derived by Dan et al. (2018)[33] for subduction plate-boundary earthquakes. The asperity area ratio S_{asp}/S derived by Eq. (1) is also in a wide range of 0.0044 to 0.11 and that by Eq. (5) is in a narrower range of 0.025 to 0.073, which is in the range of 1/2 to 2 times of $S_{asp}/S = 0.05$ derived by Dan et al. (2018)[33].

Table 7 Fault parameters of the 2003 Tokachi-oki earthquake and calculation results

outer fault parameter (F-net, 2003)	seismic moment M_0	8.21×10^{20} N·m
inner fault parameters and short-period level (Kamae and Kawabe, 2004)[24]	combined asperity area $S_{asp} = 1{,}392$ km^2	$S_{asp\,1} = 672$ km^2
		$S_{asp\,2} = 400$ km^2
		$S_{asp\,3} = 320$ km^2
	asperity stress drop $\Delta\sigma_{asp}$	$\Delta\sigma_{asp\,1} = 25$ MPa
		$\Delta\sigma_{asp\,2} = 25$ MPa
		$\Delta\sigma_{asp\,3} = 25$ MPa
	short-period level A	1.06×10^{20} N·m/s^2
results by equation (1) for a buried circular crack	averaged stress drop $\Delta\sigma$	10.5 MPa
	seismic fault area S	3,300 km^2
	asperity area ratio S_{asp}/S	0.42

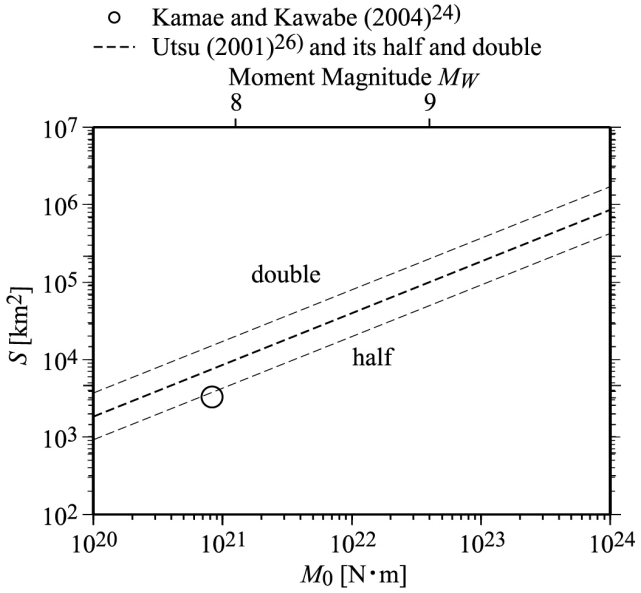

Fig. 7 Relationship between the seismic moment and the seismic fault area calculated from the inner fault parameters for the 2003 Tokachi-oki earthquake by Eq. (1) for a buried circular crack

Table 8 Fault parameters of the 2011 off the Pacific coast of Tohoku earthquake and calculation results

(a) outer fault parameter

outer fault parameter JMA [2011]	seismic moment M_0	4.22×10^{22} N·m

(b) inner fault parameters by Asano and Iwata (2012)[29] and the results

inner fault parameters and short-period level (Asano and Iwata, 2012)[29]	combined asperity area $S_{asp} = 5{,}042$ km^2	$S_{asp\,1} = 1{,}296$ km^2
		$S_{asp\,2} = 1{,}296$ km^2
		$S_{asp\,3} = 1225$ km^2
		$S_{asp\,4} = 1{,}225$ km^2
	asperity stress drop $\Delta\sigma_{asp}$	$\Delta\sigma_{asp\,1} = 23.9$ MPa
		$\Delta\sigma_{asp\,2} = 27.8$ MPa
		$\Delta\sigma_{asp\,3} = 17.5$ MPa
		$\Delta\sigma_{asp\,4} = 6.6$ MPa
	short-period level A	1.67×10^{20} N·m/s^2
results by equation (1) for a buried circular crack	averaged stress drop $\Delta\sigma$	0.09 MPa
	seismic fault area S	1,130,000 km^2
	asperity fault ratio S_{asp}/S	0.0044
results by equation (5) for a thrust fault with surface breakings	averaged dynamic stress drop $\Delta\sigma^{\#}$	0.48 MPa
	seismic fault area S	200,000 km^2
	asperity fault ratio S_{asp}/S	0.025

(c) inner fault parameters by Satoh (2012)[30] and the results

inner fault parameters and short-period level (Satoh, 2012)[30]	combined asperity area $S_{asp} = 11{,}475$ km^2	$S_{asp\,1} = 2{,}025$ km^2
		$S_{asp\,2} = 8{,}100$ km^2
		$S_{asp\,3} = 900$ km^2
		$S_{asp\,4} = 450$ km^2
	asperity stress drop $\Delta\sigma_{asp}$	$\Delta\sigma_{asp\,1} = 39.77$ MPa
		$\Delta\sigma_{asp\,2} = 25.85$ MPa
		$\Delta\sigma_{asp\,3} = 29.1$ MPa
		$\Delta\sigma_{asp\,4} = 20.57$ MPa
	short-period level A	3.51×10^{20} N·m/s^2
results by equation (1) for a buried circular crack	averaged stress drop $\Delta\sigma$	3.26 MPa
	seismic fault area S	99,800 km^2
	asperity fault ratio S_{asp}/S	0.11
results by equation (5) for a thrust fault with surface breakings	averaged dynamic stress drop $\Delta\sigma^{\#}$	1,117 MPa
	seismic fault area S	291 km^2
	asperity fault ratio S_{asp}/S	39.4*

*: invalid because of S_{asp}/S over 0.5 (Dan et al., 2011)[3].

(d) inner fault parameters by Kawabe and Kamae (2013)[31] and the results

inner fault parameters and short-period level (Kawabe and Kamae, 2013)[31]	combined asperity area $S_{asp} = 6{,}225$ km^2	$S_{asp\,1} = 1{,}600$ km^2
		$S_{asp\,2} = 2{,}500$ km^2
		$S_{asp\,3} = 441$ km^2
		$S_{asp\,4} = 784$ km^2
		$S_{asp\,5} = 900$ km^2
	asperity stress drop $\Delta\sigma_{asp}$	$\Delta\sigma_{asp\,1} = 20.4$ MPa
		$\Delta\sigma_{asp\,2} = 21.6$ MPa
		$\Delta\sigma_{asp\,3} = 15.7$ MPa
		$\Delta\sigma_{asp\,4} = 10.5$ MPa
		$\Delta\sigma_{asp\,5} = 23.1$ MPa
	short-period level A	1.71×10^{20} N·m/s^2
results by equation (1) for a buried circular crack	averaged stress drop $\Delta\sigma$	0.17 MPa
	seismic fault area S	703,000 km^2
	asperity fault ratio S_{asp}/S	0.0089
results by equation (5) for a thrust fault with surface breakings	averaged dynamic stress drop $\Delta\sigma^{\#}$	1.44 MPa
	seismic fault area S	85,100 km^2
	asperity fault ratio S_{asp}/S	0.073

(e) inner fault parameters by Kurahashi and Irikura (2013)[32] and the results

inner fault parameters and short-period level (Kurahashi and Irikura, 2013)[32]	combined asperity area $S_{asp} = 5{,}385.15$ km^2	$S_{asp\,1} = 1{,}156$ km^2
		$S_{asp\,2} = 650.25$ km^2
		$S_{asp\,3} = 1{,}806.25$ km^2
		$S_{asp\,4} = 533.61$ km^2
		$S_{asp\,5} = 1{,}239.04$ km^2
	asperity stress drop $\Delta\sigma_{asp}$	$\Delta\sigma_{asp\,1} = 16$ MPa
		$\Delta\sigma_{asp\,2} = 20$ MPa
		$\Delta\sigma_{asp\,3} = 20$ MPa
		$\Delta\sigma_{asp\,4} = 25.2$ MPa
		$\Delta\sigma_{asp\,5} = 26$ MPa
	short-period level A	1.60×10^{20} N·m/s^2
results by equation (1) for a buried circular crack	averaged stress drop $\Delta\sigma$	0.14 MPa
	seismic fault area S	823,000 Km^2
	asperity fault ratio S_{asp}/S	0.0065
results by equation (5) for a thrust fault with surface breakings	averaged dynamic stress drop $\Delta\sigma^{\#}$	1.12 MPa
	seismic fault area S	102,000 km^2
	asperity fault ratio S_{asp}/S	0.053

Figure 8 shows the relationship between the seismic moment M_0 and the seismic fault area S calculated by Eq. (1) for a buried circular crack. The figure also shows the empirical relationship by Dan et al. (2018)[33] as well as that by Utsu (2001)[26] and its half and double. Here, the empirical relationship by Dan et al. (2018)[33] is for the second- and third-stage subduction plate boundary earthquakes with surface (sea bottom) breakings and a saturated fault width, and can be applied to earthquakes with the seismic moment over 6.2×10^{21} N·m. It changes smoothly from the second stage to the third stage, and its averaged dynamic stress drop is 1 MPa.

Figure 8 indicates that the seismic fault areas calculated by Eq. (1) for a buried circular crack are 3 to 10 times larger than the empirical relationships between the seismic moment and the seismic fault area by Utsu (2001)[26] and Dan et al. (2018)[33], except for the seismic fault area from the inner fault parameters obtained by Satoh (2012)[30]. The seismic fault areas from the inner fault parameters obtained by Satoh (2012)[30] are much smaller than those from the inner fault parameters obtained by other

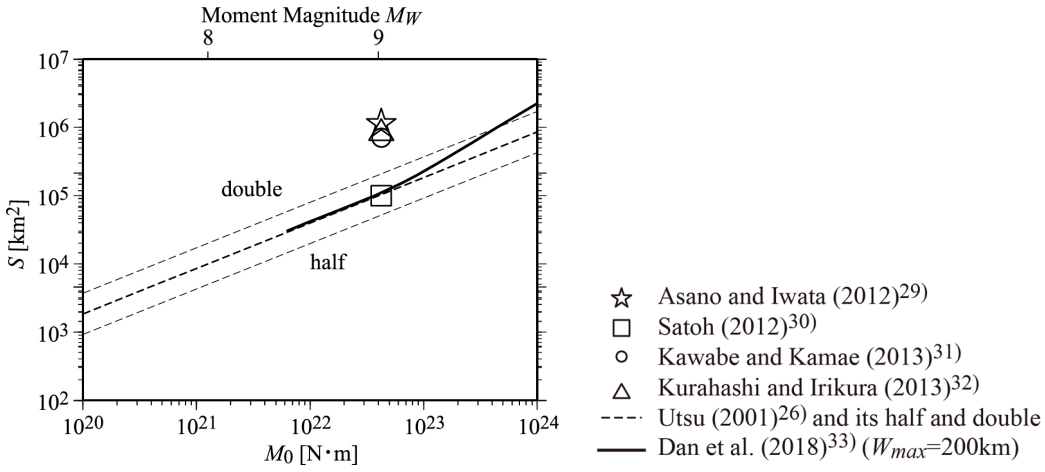

Fig. 8 Relationship between the seismic moment and the seismic fault area calculated from the inner fault parameters for the 2011 off the Pacific coast of Tohoku earthquake by Eq. (1) for a buried circular crack

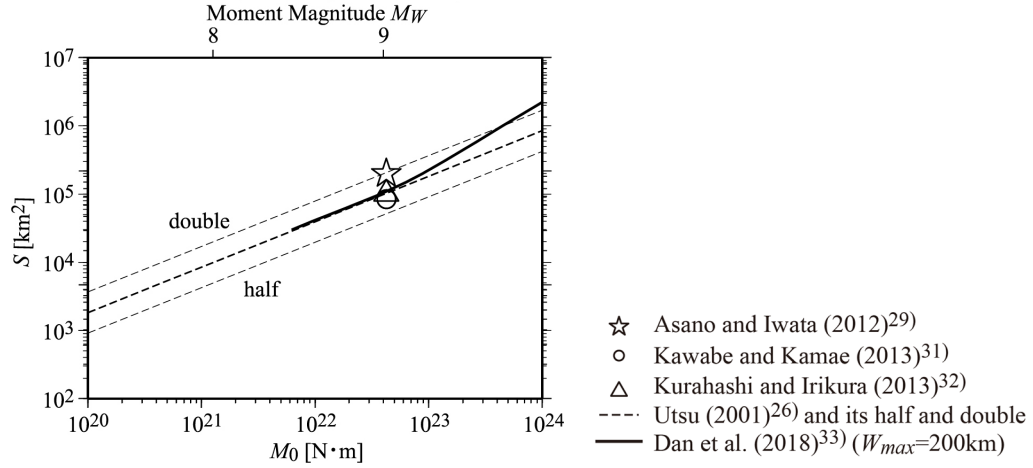

Fig. 9 Relationship between the seismic moment and the seismic fault area calculated from the inner fault parameters for the 2011 off the Pacific coast of Tohoku earthquake by Eq. (5) for a thrust fault with surface breakings

researchers. This is because the seismic fault area by Eq. (7) is inversely proportional to $(S_{aspi}\ \Delta\sigma_{aspi})^2$ and the combined asperity area S_{asp} is about twice of that obtained by other researchers and the asperity stress drop $\Delta\sigma_{aspi}$ is about 1.5 times of that obtained by other researchers.

Figure 9 shows the relationship between the seismic moment and the seismic fault area calculated by Eq. (5) for a thrust fault. Note here that we do not plot the result from the inner fault parameters of Satoh (2012)[30] because its asperity area ratio is S_{asp}/S = 39.4 and it cannot be an asperity model. The figure indicates that all the calculated seismic fault areas agree with the empirical relationships by Utsu (2001)[26] and Dan et al. (2018)[33].

Our results show that Eq. (1) for a buried circular crack might be not be valid to calculate the averaged stress drop of subduction plate-boundary earthquakes with surface (sea bottom) breakings.

5. CONCLUSIONS

We examined averaged stress drop equations, including the one for a buried circular crack, by using the seismic moments, the asperity areas, and the asperity stress drops. After we compared our calculation results with existing empirical relationships between the seismic moment and the seismic fault area, we concluded that the stress drop equation for a buried circular crack can be applied to crustal earthquakes and subduction plate-boundary earthquakes without surface (sea bottom) breakings and that other stress drop equations developed for earthquakes with surface breakings may be suitable for crustal or subduction plate-boundary earthquakes with surface breakings such as the 2016 Kumamoto earthquake and the 2011 off the Pacific coast of Tohoku earthquake.

In this paper, we examined averaged stress drop equations in terms of earthquakes without or with surface breakings. On the other hand, we experienced damaging earthquakes such as the 2000 Tottori-ken Seibu earthquake (M_W 6.6) and the 2008 Iwate-Miyagi Inland earthquake (M_W 6.9) with short fault traces. These earthquakes can be assigned between the earthquakes without surface breakings and those with surface breakings. Hence, it is necessary to obtain averaged stress drop equations applicable to this type of earthquakes.

ACKNOWLEDGMENT

The authors would like to express their appreciation to the two anonymous reviewers for their precious comments to improve the paper.

REFERENCES

1) Headquarters for Earthquake Research Promotion: Strong ground motion prediction method for earthquakes with specified source faults (“Recipe”), 2016 (in Japanese), http://www.jishin.go.jp/main/chousa/16_yosokuchizu/recipe.pdf. (last accessed on September 14, 2018)
2) Eshelby, J. D.: The determination of the elastic field of an ellipsoidal inclusion, and related problems, *Proceedings of the Royal Society of London*, Series A, Vol. 241, pp. 376–396, 1957.
3) Dan, K., Ju, D., Irie, K., Arzpeima, S. and Ishii, Y.: Estimation of averaged dynamic stress drops of inland earthquakes caused by long strike-slip faults and its application to asperity models for predicting strong ground motions, *Journal of the Structural and Construction Engineering* (*Transactions of the Architectural Institute of Japan*), No. 670, pp. 2041–2050, 2011. (in Japanese with English abstract)
4) Fujii, Y. and Matsu’ura, M.: Regional difference in scaling laws for large earthquakes and its tectonic implication, *Pure and Applied Geophysics*, Vol. 157, pp. 2283–2302, 2000.
5) Scholz, C. H.: *The Mechanics of Earthquakes and Faulting*, Second Edition, Cambridge University Press, 2002.
6) Boatwright, J.: The seismic radiation from composite models of faulting, *Bulletin of the Seismological Society of America*, Vol. 78, No. 2, pp. 489–508, 1988.
7) Knopoff, L.: Energy release in earthquakes, *Geophysical Journal of the Royal Astronomical Society*, Vol. 1, No. 1, pp. 44–52, 1958.
8) Starr, A. T.: Slip in a crystal and rupture in a solid due to shear, *Proceedings of the Cambridge Philosophical Society*, Vol. 24, pp. 489–500, 1928.
9) Watanabe, M., Sato, T. and Dan, K.: Scaling relations of fault parameters for inland earthquakes, *Proceedings of the 10th Japan Earthquake Engineering Symposium*, pp. 583–588, 1998. (in Japanese)
10) Irie, K., Dan, K., Dorjpalam, S., Kawasato, K., Ikutama, T. and Irikura, K.: Procedure for establishing asperity models for long strike-slip faults based on change in scaling laws of fault parameters. Part 3: Estimation of the formula for average dynamic stress drop by dynamic rupturing

simulation, *Summaries of Technical Papers of Annual Meeting, Architectural Institute of Japan*, Vol. B-2, pp. 103–104, 2011. (in Japanese)
11) Dorjpalam, S., Dan, K., Ju, D. and Irie, K.: Examination of the geometric constant in the average dynamic stress drop equation for long thrust faults by dynamic rupture simulation, Part 3: Asperity model simulation results, *Summaries of Technical Papers of Annual Meeting, Architectural Institute of Japan*, Vol. B-2, pp. 103–104, 2015. (in Japanese)
12) Miyake, H., Iwata, T. and Irikura, K.: Source characterization for broadband ground-motion simulation: Kinematic heterogeneous source model and strong motion generation area, *Bulletin of the Seismological Society of America*, Vol. 93, No. 6, pp. 2531–2545, 2003.
13) Shimazu, N., Muto, M., Dan, K. and Abiru, T.: Asperity models for the crustal earthquakes in Chugoku district based on short-period level by spectral inversion. Part1: 1997 Yamaguchi-Ken Hokubu earthquake, *Summaries of Technical Papers of Annual Meeting, Architectural Institute of Japan*, Vol. B-2, pp. 149–150, 2009. (in Japanese)
14) Kamae, K., Ikeda, T. and Miwa, S.: Source model composed of asperities for the 2004 Mid Niigata Prefecture, Japan, earthquake (MJMA = 6.8) by the forward modeling using the empirical Green's function method, *Earth Planets Space*, Vol. 57, pp. 533–538, 2005.
15) Maeda, T. and Sasatani, T.: Strong ground motions from an Mj 6.1 inland crustal earthquake in Hokkaido, Japan: the 2004 Rumoi earthquake, *Earth Planets Space*, Vol. 61, pp. 689–701, 2009.
16) Yoshida, S., Kagawa, T. and Noguchi, T.: Characterized seismic source model for the 2016 Central Tottori earthquake using empirical Green's function method, *Journal of the Japan Association for Earthquake Engineering*, Vol. 18, No. 2, pp. 51–61, 2018.
17) Somerville, P. G., Irikura, K., Graves, R., Sawada, S., Wald, D., Abrahamson, N., Iwasaki, Y., Kagawa, T., Smith, N. and Kowada, A.: Characterizing crustal earthquake slip models for the prediction of strong ground motion, *Seismological Research Letters*, Vol. 70, pp. 59–80, 1999.
18) Dan, K., Watanabe, M., Sato, T. and Ishii, T.: Short-period source spectra inferred from variable-slip rupture models and modeling of earthquake faults for strong motion prediction by semi-empirical method, *Journal of Structural and Construction Engineering* (*Transactions of the Architectural Institute of Japan*), No. 545, pp. 51–62, 2001. (in Japanese with English abstract)
19) Irikura, K., Miyakoshi, K., Kamae, K., Yoshida, K., Somei, K., Kurahashi, S. and Miyake, H.: Applicability of source scaling relations for crustal earthquakes to estimation of the ground motions of the 2016 Kumamoto earthquake, *Earth Planets Space*, doi:10.1186/s40623-016-0586-y, 2017.
20) Headquarters for Earthquake Research Promotion: National Seismic Hazard Maps of Japan 2014 edition, 2014.
21) Satoh, T.: Broadband source characteristics of the 2016 Kumamoto earthquake estimated from strong motion records, *Journal of the Structural and Construction Engineering (Transactions of the Architectural Institute of Japan)*, Vol. 82, No. 741, pp. 1707–1717, 2017. (in Japanese with English abstract)
22) Oana, A., Dan, K., Miyakoshi, J., Fujiwara, H., Morikawa, N. and Maeda, T.: Estimation of characterized source model of the mainshock in the 2016 Kumamoto earthquakes using the stochastic Green's function method, *Japan Geoscience Union Meeting*, SCG70-P04, 2017.
23) Aoi, S., Honda, R. Morikawa, N. Sekiguchi, H. Suzuki, H. Hayakawa, Y. Kunugi, T. and Fujiwara, H.: Three-dimensional finite difference simulation of long-period ground motions for the 2003 Tokachi-oki, Japan, earthquake, *Journal of Geophysical Research*, Vol. 113, B07302, doi:10.1029/2007JB005452, 2008.
24) Kamae, K. and Kawabe, H.: Source modeling of the 2003 Tokachi-oki earthquake and verification of the recipe for strong ground motion prediction, *Summaries of Technical Papers of Annual Meeting*, *Architectural Institute of Japan*, Vol. B-2, pp. 519–520, 2004. (in Japanese)
25) Kanamori, H. and Anderson, D. L.: Theoretical basis of some empirical relations in seismology, *Bulletin of the Seismological Society of America*, Vol. 65, No. 5, pp. 1073–1095, 1975.
26) Utsu, T.: *Seismology,* 3rd ed**.**, Kyoritsu Shuppan, 2001. (in Japanese)
27) Somerville, P. G., Sato, T., Ishii, T., Collins, N. F., Dan, K. and Fujiwara, H.: Characterizing heterogeneous slip models for large subduction earthquakes for strong ground motion prediction,

Proceedings of the 11th Japan Earthquake Engineering Symposium, pp. 163–166, 2002. (in Japanese)
28) Yoshida, K., Miyakoshi, K. and Irikura, K.: Source process of the 2011 off the Pacific coast of Tohoku earthquake inferred from waveform inversion with long-period strong-motion records, *Earth Planets Space*, Vol. 63, pp. 1–5, 2011.
29) Asano, K. and Iwata, T.: Source model for strong ground motion generation in the frequency range 0.1-10 Hz during the 2011 Tohoku earthquake, *Earth Planets Space*, Vol. 64, pp. 1111–1123, 2012.
30) Satoh, T.: Source modeling of the 2011 off the Pacific coast of Tohoku earthquake using empirical Green's function method and the scaling law of the source parameters, *Journal of the Structural and Construction Engineering (Transactions of the Architectural Institute of Japan)*, Vol. 77, No. 675, pp. 695–704, 2012. (in Japanese with English abstract)
31) Kawabe, H. and Kamae, K.: Source modeling of the 2011 off the Pacific coast of Tohoku earthquake, *Journal of the Japan Association for Earthquake Engineering*, Vol. 13, No. 2, pp. 75–87, 2013. (in Japanese with English abstract)
32) Kurahashi, S. and Irikura, K.: Short-period source model of the 2011 Mw 9.0 off the Pacific coast of Tohoku earthquake, *Bulletin of the Seismological Society of America*, Vol. 103, No. 2B, pp. 1373–1393, 2013.
33) Dan, K., Ju, D., Dorjpalam, S., Irie, K., Suzuki, S., Fujiwara, H. and Morikawa, N.: Procedure of evaluating fault parameters of subduction plate-boundary earthquakes with surface fault breakings for strong motion prediction, *IAEA Second Workshop on Best Practices in Physics-based Fault Rupture Models for Seismic Hazard Assessment of Nuclear Installations: Issues and Challenges towards Full Seismic Risk Analysis*, Cadarache-Chateau, France, May 14–16, 2018.

(Original Japanese Paper Published: September, 2019)
(English Version Submitted: January 9, 2020)
(English Version Accepted: February 19, 2020)